

Dynamical Matching of Josephson Vortex Lattice with Sample Edge in Layered High- T_c Superconductors: Origin of the Periodic Oscillation of Flux Flow Resistance

M. Machida

*CCSE, Japan Atomic Energy Research Institute, 6-9-3 Higashi-Ueno, Taito-ku Tokyo 110-0015, Japan
and Materials Science Division, Argonne National Laboratory, 9700 S. Cass Avenue Argonne, Illinois 60439*

(Received 12 December 2001; published 23 January 2003)

We numerically investigate Josephson vortex flow states in layered high- T_c superconductors motivated by a recent experimental observation for accurate periodic magnetic field dependences of the Josephson vortex flow resistance over a wide range of magnetic field (0.5–4.0 T). We confirm in our mesoscale simulations that dynamical matching of Josephson vortex lattice with sample edge is responsible for the periodic dependence. The present simulations reveal that the Josephson vortex lattice flow speed is particularly suppressed when the moment of vortex entry matches that of vortex escape. Thus, the possible matching situations are taken into account and the observed periodicity is successfully explained.

DOI: 10.1103/PhysRevLett.90.037001

PACS numbers: 74.50.+r, 74.25.Qt, 74.78.Fk, 74.78.Na

Recently, elastic and plastic motions of superconducting vortices in type II superconductors have been intensively investigated under the presence of the periodic [1] and nonperiodic potentials [2] quenched on superconducting substrates. Since the moving vortices collectively interact with those potentials, many rich dynamical phases are expected [1,2]. Especially, the periodic pinning potential gives rise to drastic dynamical matching effects [1] which offer a new kind of superconducting devices. In this Letter, we consider a novel type of dynamical matching effect in Josephson vortex flow states in layered high- T_c superconductors. The matching is an intrinsic one with sample edges without any artificial arrangements for pinning sites.

The highly anisotropic layered high- T_c superconductors represented by $\text{Bi}_2\text{Sr}_2\text{CaCu}_2\text{O}_8$ (Bi-2212) are regarded as intrinsic Josephson stacked array systems [3] in which the layer parallel magnetic field penetrates into the junction area as Josephson vortex [4]. In Josephson vortex dynamics there are some peculiar points [5] in contrast to Abrikosov and pancake vortices. For a driving force exerted on the c axis, the so-called intrinsic pinning strongly prevents the motion along the c axis [6], while the sliding motion along the ab plane is easily driven under the presence of the c -axis transport current [7]. Moreover, the core pinning mechanism is useless since the Josephson vortex is coreless [4]. Thus, the Josephson vortex is believed to be almost transparent on various quenched potentials under the c -axis parallel current. On the other hand, we suggest that sample edges should specifically have an important role as barriers for Josephson vortex motions. This is because the vortex current distribution remarkably changes only at moments of its entry and escape at sample edges. Of course, such edge effects should become not effective with increasing the sample dimension because these are screened by bulk properties. Thus, we study dynamical matching of the

Josephson vortex lattice with the sample edges in mesoscale systems.

Very recently, a strikingly regular periodic dependence of Josephson vortex flow resistance on the layer parallel magnetic field has been reported in mesoscale layered high- T_c superconducting Bi-2212 sample [8]. The periodic dependence can be very distinctly observed over a wide range of the field (0.5–4.0 T), and its periodicity is not dependent on the magnetic field at all. The measured periodicity H_p is given by a relation $\frac{\phi_0}{2LD}$ where ϕ_0 , L , and D are the flux quanta, the sample width perpendicular to the layer parallel field, and the layer periodicity along the c axis, respectively. Moreover, it is now known that there are some experimental conditions required for the clear detection of the regularity: (i) The upper limit of the applied c -axis transport current is about $0.1j_c$ and the periodic structures become unclear with increasing the current; (ii) the sample dimension is limited within $L < 30 \mu\text{m}$. In this Letter, we reproduce these experimental results by performing realistic numerical simulations and consequently clarify that the periodic structure can be ascribed to the matching of the Josephson vortex lattice with the sample edges. Moreover, we connect the result with a static Fraunhofer pattern and suggest possible device applications.

Although there have been some arguments about lattice configurations of static Josephson vortices in Bi-2212 [9], it is reasonable to expect flow states of the densely packed triangular lattice to be steady states under the relatively high field ($\sim T$) and the tiny c -axis transport current. This assumption allows us to considerably reduce calculation efforts since the calculation in two successive stacked junctions can represent the total system dynamics by the application of the periodic boundary condition on the c -axis direction as schematically seen in Fig. 1(I). The equation employed in numerical simulations is given as

$$\beta \frac{\partial \varphi_{\ell+1,\ell}}{\partial t'} - \frac{\partial^2 \varphi_{\ell+1,\ell}}{\partial x'^2} + \sin \varphi_{\ell+1,\ell} = \frac{\lambda_{ab}^2}{D^2} \Delta^{(2)} \left(\beta \frac{\partial \varphi_{\ell+1,\ell}}{\partial t'} + \sin \varphi_{\ell+1,\ell} \right), \quad (1)$$

where $\varphi_{\ell+1,\ell} [\equiv \theta_{\ell+1}(t) - \theta_\ell(t) - \frac{2e}{\hbar c} \int_{\ell D}^{(\ell+1)D} dz A_z(z, t)]$ is the gauge invariant phase difference, $\Delta^{(2)}$ stands for a difference as $\Delta^{(2)} f_{\ell+1,\ell} = f_{\ell+2,\ell+1} + f_{\ell,\ell-1} - 2f_{\ell+1,\ell}$, λ_{ab} the penetration depth in the ab plane, and β is related with the McCumber parameter as $\beta = 1/\sqrt{\beta_c}$ [10,11]. The time and space in Eq. (1) is rescaled as $t' = \omega_p t$, where ω_p is the Josephson plasma frequency and $x' = 1/\lambda_c x$ where λ_c is the c -axis penetration depth. This equation is derived from the Maxwell equation without the displacement current and the Josephson relations for time and space. The exclusion of the displacement current does not give propagating plasma waves. In the notable current range the flux flow motions do not resonate with the plasma waves due to much slower flow speed than that of the propagating plasma wave. On the other hand, in the resonant region, the high speed flux motion smears the edge effects. Thus, the edge effect and the plasma resonance do not work cooperatively. In the numerical simulation of Eq. (1), the current and the magnetic field are applied by the boundary condition of Eq. (1) at both sample edges as $\partial \varphi_{\ell+1,\ell} / \partial x|_{\text{edge}} = H_a \pm 0.5 i_a L$, where H_a , i_a , and L are the applied magnetic field, the applied current, and the sample size perpendicular to the magnetic field, respectively [11], and $+(-)$ indicates the condition at the right (left) edge.

Let us show simulation results. Figure 1(II) presents the magnetic field dependence of the voltage measured for three c -axis constant current values. These results clearly indicate that the flux flow voltage periodically oscillates over a wide range of the magnetic field. Moreover, if the applied current is reduced, the periodic structures are found to become more remarkable especially in the low field range. These behaviors are consistent with experimental results although our oscillation amplitudes are relatively smaller than those of experimental results due to elimination of the in-plane dissipation which may amplify the oscillation [12].

The sample size effect on the oscillating behavior of the flux flow voltage is shown in Fig. 2(I), where simulation results for three sizes are displayed. From Fig. 2(I) it is clearly found that the periodicity decreases and the periodic structure becomes unclear with increasing the size. These tendencies are also consistent with the experiment. Furthermore, the size dependence of the periodicity H_p obtained from both the experiments [8] and the simulations lie on the expected line expressed by the relation $H_p = \frac{\phi_0}{2LD}$, as seen in Fig. 2(II). Thus, it is found that the present simulations successfully reproduce the experimental results.

Now, let us clarify an origin of the periodic dependence on the magnetic field. At first, we examine whether the edge barrier works effectively in the simulations. The local voltage measurements as shown in Fig. 3(I) can be easily performed in this numerical simulation in contrast

to difficulties in experiments. The time evolutions of three local voltages at the left edge, the right edge, and the center site are measured as indicated in Fig. 3(I) for a comparison between vortex dynamics at the edges and the center region. The figures (a), (b), and (c) in Fig. 3(II) are the time developments of these local voltages, respectively. At the left edge vortices exit while these penetrate at the right edge. The sharp peak structures are found in time developments of the all local voltages [Fig. 3(II)(a–c)]. These peaks arise from vortex centers passing through the measuring points because the local voltage is given as $V_{\ell+1,\ell}(x, t) = -\frac{2\pi c}{\phi_0} v_L \partial_x \varphi_{\ell+1,\ell}(x, t)$, where v_L is the vortex velocity, and the spatial derivative $\partial_x \varphi_{\ell+1,\ell}(x, t)$ is sharply modulated in the vortex center [4]. From a comparison between $V_{2L}(t)$, $V_{2R}(t)$ at both edges and $V_{2C}(t)$ at the center, it is found that the voltage peak amplitudes at both edges are about 2 times larger than that at the center site. This difference can be understood as follows. In both edges, suppose that local barrier potentials exist as schematically shown in Fig. 3(III). Once a vortex reaches the top of the potential, the vortex speeds up in a downward direction. Thus, it is found that effective barriers on the vortex dynamics actually exist at both edges.

Next, let us investigate how the edge barrier causes the periodic dependence of the flow resistance. We measure time developments of three local voltages $V_{2L}(t)$, $V_{2R}(t)$,

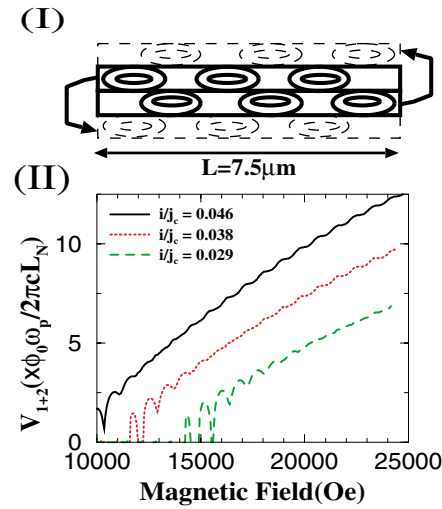


FIG. 1 (color online). (a) The schematic figure for the simulated region. The periodic boundary condition along the c -axis is imposed. The arrows and the dashed lines schematically depict the image of the periodic boundary condition. (b) The simulation results of the magnetic field dependences of dc voltage measured in two stacked junctions V_{1+2} for three different c -axis currents. The sample dimension L is $7.5 \mu\text{m}$. L_N means the mesh number along the ab plane in the simulation ($L_N = 200$).

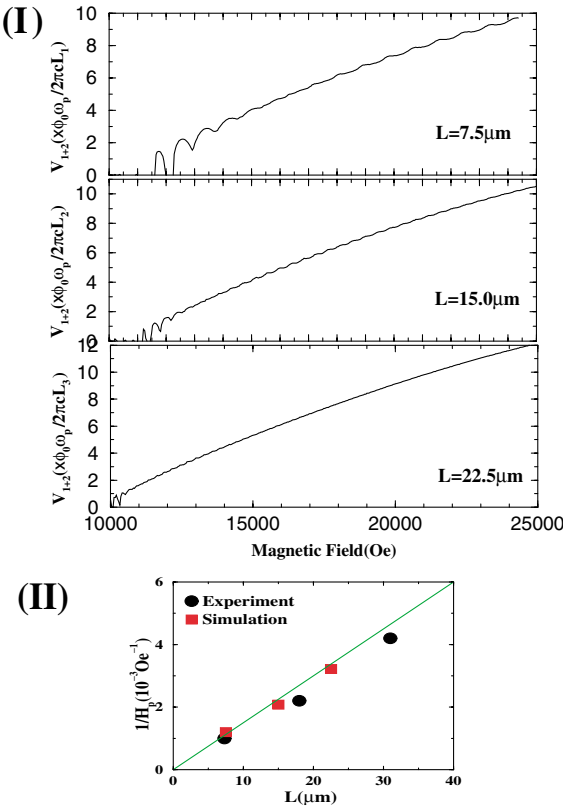


FIG. 2 (color online). The sample size effect on the magnetic field dependence of the flux flow voltage for a current $j/j_c = 0.038$. (I) The magnetic field dependences of the flux flow voltage measured in two stacked junctions for three size $L = 7.5, 15.0$, and $22.5 \mu m$. (II) The comparison of the periodicity H_p between the experiment [8] and the simulation in different sample sizes. The straight line indicates the relation $H_p = \frac{\phi_0}{2LD}$

and $V_{1R}(t)$ for three points (a), (b), and (c) in the magnetic field dependence of the flux flow voltage given in Fig. 4(I). Figures 4(a)–4(c) show the time developments of these local voltages in the three points (a), (b), and (c), respectively. In these figures [Figs. 4(a)–4(c)], the left panel compares the time development of the local voltage $V_{2L}(t)$ with that of $V_{2R}(t)$, while the center panel compares $V_{2L}(t)$ with $V_{1R}(t)$. In the minimum point (a) as seen in Fig. 4(I), it is found from the left panel of Fig. 4(a) that the moment of the vortex entry completely coincides with that of the escape in the same upside junction while the entry and the escape for the upside and the downside junction occur in an alternating manner as seen in the center panel of Fig. 4(a). Thus, the moment of the dynamical matching of the Josephson vortex lattice with the edges in the minimum point (a) is schematically displayed in the right panel of Fig. 4(a). In the next minimum point (c), it is found that the moment of the vortex escape in the upside junction coincides with that of the entry in the downside junction from the center panel in Fig. 4(c), while those for the same upside junction do not coincide as seen in the left panel in Fig. 4(c). The matching moment in the minimum point (c) is also schemati-

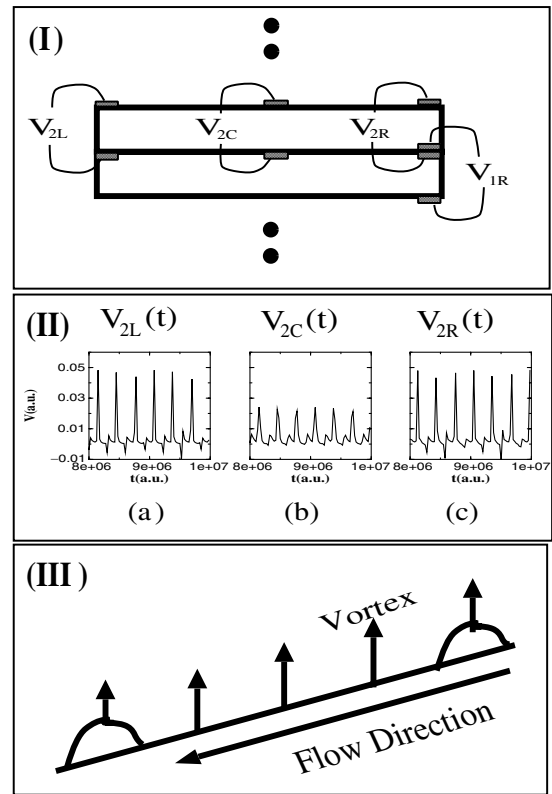


FIG. 3. (I) The schematic view for the local voltage measurements performed in the simulation. (II) The time evolutions of the local voltages, (a) $V_{2L}(t)$, (b) $V_{2C}(t)$, and (c) $V_{2R}(t)$ whose measuring positions are indicated in (I). (III) The schematic figure for the free energy potential in the Josephson vortex flow state under the presence of the edge barrier potential.

cally shown in the right panel in Fig. 4(c). On the other hand, at the maximum point (b) it is found from Fig. 4(b) that such matching at edges is never observed. Thus, these results reveal that the vortex moving velocities show the minimum at the magnetic field in which the vortex entry and escape occur at the same time. Let us explain why the matching reduces the vortex velocities. In such matching conditions, two vortices per two junctions simultaneously feel the edge barrier potential as seen in the right panels of Figs. 4(a) and 4(c), while in nonmatching conditions only a vortex per two junctions receives the potential. Thus, it is found that the vortex lattice motion suffers more enhanced friction in the matching conditions. In fact, the vortex velocity difference between the minimum and the maximum points can be checked by counting the number of peaks per the same time width for the matching cases (a) and (c) and the nonmatching case (b). In addition, we can derive the magnetic field periodicity H_p according to the schematic panels of Figs. 4(a) and 4(c) as follows: When the state reaches from (a) to (c) with increasing the magnetic field the penetration of a half of vortex per each junction is required. Consequently, the periodicity is given by $H_p = \frac{\phi_0}{2LD}$. We note that this result is characteristic to the triangular flux lattice configuration appearing in stacked junction systems. On the other

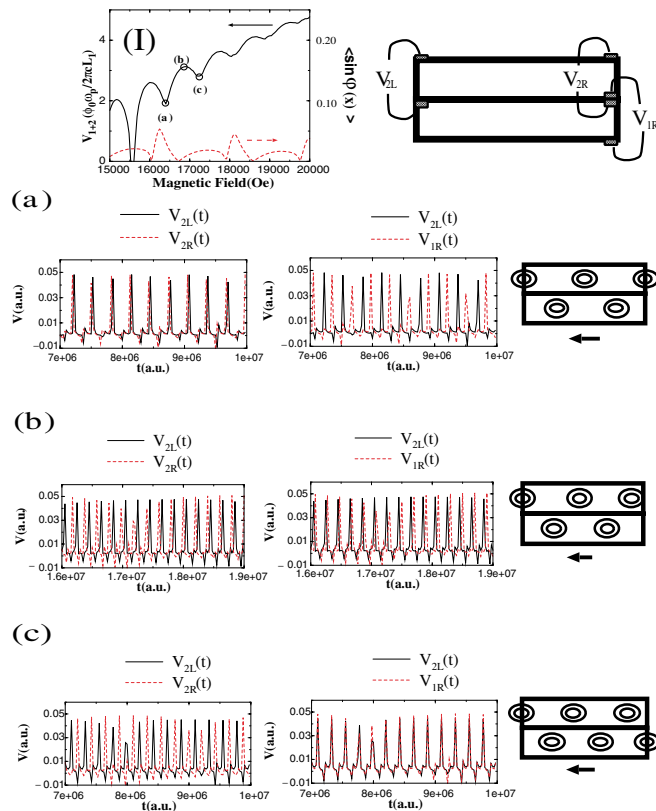


FIG. 4 (color online). The comparisons among the time developments of the local voltages at the three edges (see the upper right panel) for the two minimum points (a),(c) and the one maximum point (b) in (I) the magnetic field dependence of the flux flow voltage. In (a)–(c), the left panel gives a comparison between $V_{2L}(t)$ and $V_{2R}(t)$, the center panel contrasts $V_{2L}(t)$ with $V_{1R}(t)$, and the right panel schematically depicts the corresponding matching moment.

hand, the matching periodicity in the single junction is given by $H_p = \phi_0/L(D + 2\lambda_L)$, where λ_L is London penetration depth [13]. Furthermore, we note that there is a connection between the oscillation in the dynamical case and the so-called Fraunhofer pattern in the static case without the applied current. In Fig. 4(I), $J_c^{\max}(B) = \frac{1}{LN} |\sum_\ell \int^L dx \sin \varphi_{\ell+1,\ell}(x)|$, where N is the number of the stacked layers, is given by the dashed line [14]. From a comparison between the magnetic field dependence of the flow voltage and $J_c^{\max}(B)$, it is found that the oscillation minimum almost coincides with the maximum point in $J_c^{\max}(B)$. This result just reflects that the amount of the supercurrent supply in the superconducting (static) state is closely connected with the (edge) pinning strength on the vortex lattice flow.

In conclusion, the Josephson vortex strongly feels the sample edge barrier because the current core shape sharply changes at the moment of the entry and the escape. Therefore, the Josephson vortex lattice shows the considerable matching with sample edges and consequently gives the accurate periodic oscillation of the flow resistance over the wide range of the magnetic field.

This remarkable character is applicable to a flux SQUID meter under the high magnetic field and a voltage amplifier with the field control [15]. In the former case the local field variation under the strong background field is easily detected by monitoring the voltage modulation [15], while the latter case may be used as a system embedded in magnetic field of about 1 T produced by permanent magnets [15]. Moreover, these systems can work up to fairly high temperature compared to those using conventional Josephson junctions [8]. Thus, we propose that the Josephson vortex flow states in the mesoscale layered high- T_c superconductors are very promising for various device applications.

The author thanks K. Hirata, S. Ooi, A. E. Koshelev, T. Yamashita, T. Koyama, and N. Sasa for illuminating discussions, and CREST(JST) for financial supports. In Argonne, this work was supported by the U. S. DOE, Office of Science, under Contract No. W-31-109-ENG-38.

- [1] For example, see C. Reichhardt *et al.*, Phys. Rev. B **64**, 144509 (2001), and many references therein.
- [2] For example, see C. J. Olson *et al.*, Phys. Rev. B **64**, 140502(R) (2001); C. J. Olson *et al.*, Phys. Rev. Lett. **81**, 3757 (1998), and many references therin.
- [3] R. Kleiner *et al.*, Phys. Rev. Lett. **68**, 2394 (1992); G. Oya *et al.*, Jpn. J. Appl. Phys. **31**, L829 (1992).
- [4] J. R. Clem and M. W. Coffey, Phys. Rev. **42**, 6209 (1990).
- [5] For example, see R. Kleiner, Phys. Rev. B **50**, 6919 (1994); M. Machida *et al.*, Physica (Amsterdam) **330C**, 85 (2000); A. E. Koshelev and I. S. Aranson, Phys. Rev. Lett. **85**, 3938 (2000).
- [6] M. Tachiki and S. Takahashi, Solid State Commun. **70**, 291 (1989).
- [7] See A. Irie *et al.*, Appl. Phys. Lett. **72**, 2159 (1998). The vortex speed can reach to the velocity of the highest plasma mode ($1.5\text{--}1.8 \times 10^6$ m/s).
- [8] S. Ooi, T. Mochiku, and K. Hirata, Phys. Rev. Lett. **89**, 247002 (2002).
- [9] B. I. Ivlev *et al.*, J. Low Temp. Phys. **80**, 187 (1990); L. Balents *et al.*, Phys. Rev. B **52**, 12951 (1995); X. Hu *et al.*, Phys. Rev. Lett. **85**, 2577 (2000).
- [10] See A. Barone and G. Paterno, *Physics and Application of the Josephson Effect* (Wiley, New York, 1982), and references therein.
- [11] M. Machida *et al.*, Physica (Amsterdam) **330C**, 85 (2000).
- [12] For the in-plane dissipation, see A. E. Koshelev, Phys. Rev. B **62**, R3616 (2000). The inclusion of the in-plane dissipation does not qualitatively change the present results.
- [13] Generally, the edge matching effect has been studied in the context of Fiske resonance in single junctions rather than the periodic character of the flow resistance; see [10]. In addition, we note in stacked junction systems that $H_p = \frac{\phi_0}{LD}$ if the lattice configuration is square.
- [14] We note that $J_c^{\max}(B)$ is calculated from Eq. (1) without the current.
- [15] T. Yamashita (private communication).